

A MONTE CARLO STUDY ON BEAM MODIFIER DESIGN FOR TOTAL SKIN ELECTRON IRRADIATIONS

Sung-Joon Ye

Department of Radiation Oncology/Physics
University of Alabama at Birmingham
1824 6th Ave. S.
Birmingham, AL 35294 USA
sye@uab.edu

ABSTRACT

We used Monte Carlo (MC) techniques as a guide in the beam modifier design of our Total skin electron irradiation (TSEI) system. By matching MC simulations to standard beam measurements at 100 cm Source-to-Surface-Distance (SSD), the parameters of primary electrons were determined to be mono-energetic at 6.72 MeV, parallel, and circular beams having a Gaussian radial distribution with FWHM = 0.13 cm. They were then used to simulate our TSEI unit with eight sets of energy degraders and flattening filters. An energy degrader of a 0.6 cm-thick PMMA plate, blacking a jaw-shaped field (40 cm × 40 cm) at 100 cm SSD, showed the best performance in terms of dose rate and uniformity. A flattening filter, consisting of a 12 cm × 12 cm aluminum plate of 0.6 cm-thickness and placed just behind the energy degrader was considered optimal. Such optimized combination produced a beam that was flat within ±3% up to 60 cm off-axis distance, dropped by not more than 6% at a distance of 90 cm, and had an x-ray contamination of < 3%. The maximum dose of a stationary phantom occurred at 0.65 cm-depth, while the maximum dose of a rotating phantom at the surface. The surface dose of the rotating phantom was approximately 40% of the maximum dose of the stationary phantom. By evaluating the dosimetric performance of beam modifier designs for TSEI, the Monte Carlo simulations reduced the costly efforts that could, otherwise, result from constructing and measuring a number of prototypes.

Key Words: Total Skin Electron Irradiations, Flattening Filter, Energy Degradation, Dosimetry

1 INTRODUCTION

Malignant skin diseases, such as mycosis fungoides and cutaneous lymphomas, are often treated with total skin electron irradiation (TSEI) [1]. Techniques and dosimetry for TSEI have been developed by individual medical physicists, and thus vary from clinic to clinic. Some of these techniques are described in the AAPM Report No. 23 entitled “Total Skin Electron Therapy: Technique and Dosimetry” [2]. Nominal beam energies are typically 4 – 10 MeV at the accelerator beam exit window, and are reduced by energy degraders to have d_{\max} (depth of maximum dose) near or at the skin surface. It is recommended to have available field sizes of 200 cm in height and 80 cm in width, with dose uniformity of ± 8% in height and ± 4% in width over the central 160 cm × 60 cm area. Despite the extended source-to-surface-distance (SSD) required to obtain such large field sizes, the dose rate at the patient should be larger than 10 cGy/min, and bremsstrahlung x-ray contamination should be lower than 5%.

To achieve the recommended beam characteristics, energy degraders and flattening filters have to be developed for the specific accelerator and treatment distance. Traditionally, these

procedures have been done by series of experiments [3-7]. Antolak et al. [8] used a multiple scattering theory to design their TSEI beam. More recently, Pavón et al. [9] demonstrated the capability of Monte Carlo (MC) simulations to evaluate the beam properties of their TSEI unit. In this paper we describe Monte Carlo simulations that were used in the design of a novel type of energy degrader and flattening filter, and to obtain the beam characteristics of our TSEI system. Depth dose curves are presented for stationary beams as well as treatments where the patient stands on a rotating platform.

1.1 Description of the TSEI Unit at UAB

Our TSEI unit is based on the 6 MeV electron beam from a Clinac 2100C medical accelerator, serial #78, with Type-III dual internal scattering foil system, operating in the high dose rate (HDTS) mode (Varian Medical Systems, Inc., Palo Alto, CA). The treatment head geometry is the same as in the standard 6 MeV electron mode, but no other electron applicator is used. The HDTS insert is electronically interlocked to open the upper and lower jaws to their maximum field size, 40 cm \times 40 cm projected to 100 cm SSD. During treatment, collimator and gantry are turned to 135° and 315°, respectively. This arrangement produces a horizontal beam having one of the diagonals vertical for maximum field height. A square flattening filter is placed at isocenter (SSD = 100 cm), perpendicular to the beam axis.

The patient is standing at the center of a turntable having its axis of rotation at 297 cm from isocenter, rotating at a rate of 15 sec per revolution. Since the patient turns many revolutions (30 revolutions or more) during the 6 – 7 min it takes to deliver a typical dose of 100 cGy per fraction, the dose around the circumference is sufficiently uniform so that it is not necessary to synchronize the rotation with the initiation and termination of the beam. Figure 1 shows the schematic diagram for the rotational TSEI unit at the UAB comprehensive cancer center.

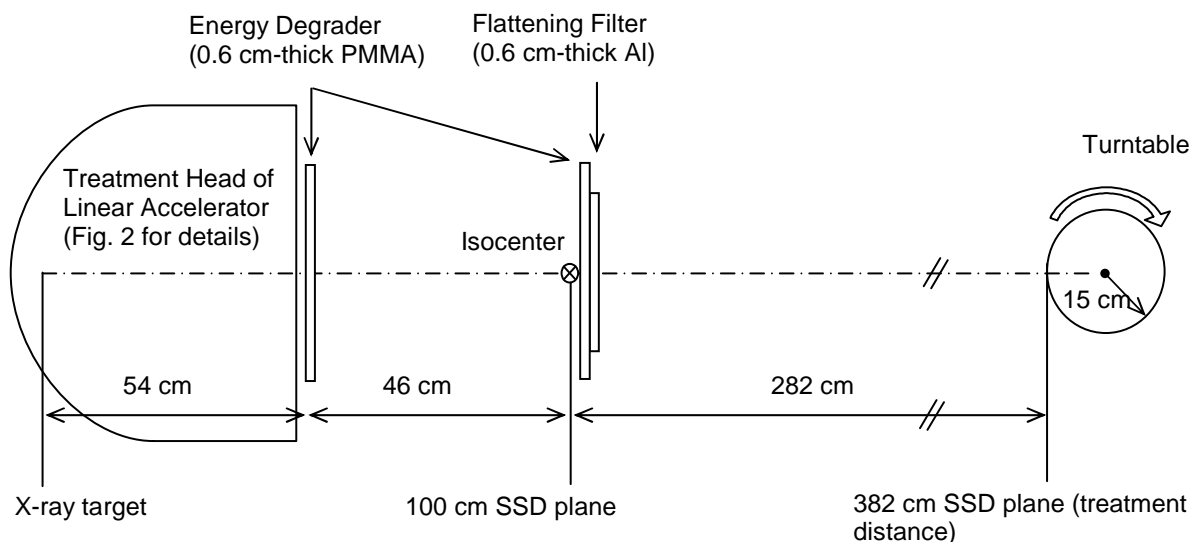


Figure 1. Schematic diagram of the total skin electron irradiation (TSEI) unit at the University of Alabama at Birmingham. The patient, on a turntable, is treated with a single electron field from a linear accelerator. The energy degrader is located at either of two positions arrowed.

1.2 Monte Carlo Simulations

Our simulations needed to take into account all major components of the treatment head, the energy degrader, and flattening filter. The EGS4 [10] user code BEAM [11], which provides numerous predefined component modules, can be readily used for the simulations. The BEAM code (version Year 2002) with the PRESTA algorithm [12] seemed best suited for this study. Our EGS4/BEAM simulations consisted of two major steps. The first step involved adjusting the primary electron beam parameters to match the beam data measured at 100 cm SSD. The so found beam parameters were then used to compute dose distributions at the treatment distance of 382 cm SSD for eight sets of energy degraders and flattening filters (see Table I), and thereby provide guidance for the manufacturing of an optimized beam modifier. The construction details of the treatment head were provided by the manufacturer. Figure 2 shows a schematic of the accelerator treatment head assumed in our EGS4/BEAM simulations.

Using the EGS4/BEAM code, two phase space files were generated, one in a plane at 85 cm SSD and one at 382 cm SSD (at the patient's skin). Each of the phase space files contained spatial, spectral, and angular distributions of electrons, photons, and positrons. In all BEAM simulations, 1×10^8 primary electrons were transported from the exit window of the wave guide to 100 cm SSD for the 85 cm SSD phase space, and to 400 cm SSD for the 382 cm SSD phase space. Such extra transportation beyond the phase space planes eliminates potential artifacts due to boundary effects. Simulations typically took 20 h – 24 h CPU time on our 2.4 GHz Linux-based computer. The 1×10^8 primary histories scored about 4.5×10^7 particles in the phase space at 85 cm SSD, and about 2.0×10^7 particles at 382 cm SSD.

Table I. Construction of energy degraders and flattening filters investigated using the Monte Carlo simulations. The labels in the first column are for later reference.

Label of Beam Modifiers	PMMA Energy Degradar (ED)		Aluminum Flattening Filter (FF)	
	Dimension, cm	SSD, cm	Dimension, cm	SSD, cm
<i>BM1</i>	25×25×0.6	54	20×20×0.6	100
<i>BM2</i>	25×25×0.6	54	15×15×0.6	100
<i>BM3</i>	25×25×0.6	54	12×12×0.6	100
<i>BM4</i>	30×30×0.6	100	12×12×0.6	100.6
<i>BM5</i>	50×50×0.6	100	12×12×0.6	100.6
<i>BM6</i>	40×40×0.6	100	12×12×0.6	100.6
<i>ED only</i>	25×25×0.6	54		
<i>FF only</i>			12×12×0.6	100

An EGS4 user code, DOSXYZ [13] was used to calculate dose distributions in a 60 cm × 60 cm × 30 cm water phantom at 100 cm SSD, irradiated by the 85 cm SSD phase space determined in the previous simulations. In all DOSXYZ simulations, 4×10^8 particles were sampled from the 85 cm SSD phase space file, yielding dose distributions in the water phantom at 100 cm SSD with statistical uncertainties of $< \pm 2\%$. The doses in the region of interest were scored in voxels of 0.5 cm (width) × 2.0 cm (length) × 0.1 cm (depth). Such large numbers of particles required recycling the phase space file, but the number of recycles was less than 10.

Another EGS4 user code, DOSRZ [14], was used to calculate stationary and rotational depth dose distributions in a cylindrical water phantom located at the treatment position of the patient.

The cylinder had a radius of 15 cm, a length of 50 cm, and had flat top and bottom surfaces. It was irradiated by the 382 cm SSD phase space at 382 cm SSD, having its axis oriented perpendicular as well as parallel to the beam direction. The perpendicular orientation simulated the treatment of a rotating patient (rotational depth doses), whereas the parallel orientation provided depth doses at 382 cm SSD in a stationary flat phantom (stationary depth doses). In the DOSRZ simulations, doses for the parallel orientation were tallied in cylindrical plates of 1 mm thickness from surface to 1 cm-depth and of 2.5 mm thickness between 1 cm- and 10 cm-depth, providing the familiar depth dose curves. For the orthogonal orientation, doses were tallied in 1.0 mm thick concentric cylindrical shells from the surface to 1 cm-depth and in 2.5 mm thick concentric cylindrical shells between 1 cm- and 10 cm-depth. Since in a rotating phantom each point in a given shell assumes all azimuthal angles during rotation, the dose at a given depth is equal to the average dose in the corresponding shell of a stationary phantom. Hence it was not necessary to simulate the rotational motion of the phantom. Only 1×10^6 particles had to be sampled from the 382 cm SSD phase space file to achieve the statistical uncertainty of $< \pm 2\%$ for dose distributions in the stationary cylinder having the axis aligned with the beam axis, and the rotating cylinder having its axis perpendicular to the beam. There was no need to recycle the phase space file in these simulations.

Following recently published papers [15-20], the cut-off energies for particle transport were set to $P_{cut} = 0.01$ MeV for photons and $E_{cut} = 0.7$ MeV for electrons/positrons. Similarly, the threshold energies for bremsstrahlung creation and secondary electron creation were set to $AP = 0.01$ MeV and $AE = 0.7$ MeV, respectively. No variance reduction techniques were applied. The default PRESTA parameters [12] were used for the electron step size.

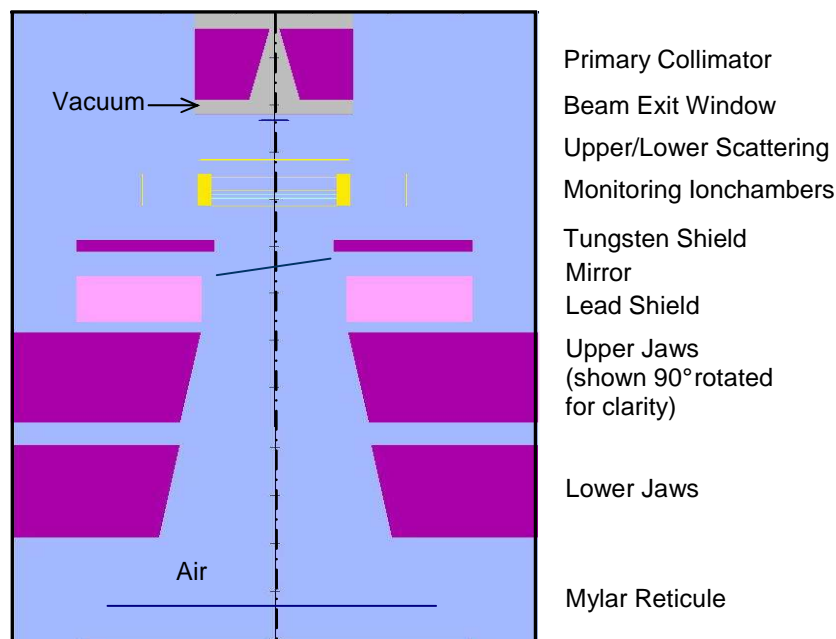


Figure 2. Schematic diagram of the accelerator treatment head assumed in Monte Carlo simulations using EGS4/BEAM [11]. The Lower Jaws are turned 90° for clarity.

2 RESULTS

2.1 Primary Electron Beam Parameters for Monte Carlo Modeling

The depth doses are affected primarily by the electron energy, E_0 , while beam width and divergence have virtually no influence. The calculated values of d_{\max} , R_{50} , and R_p agreed with measured data within 1 mm when a primary energy of 6.72 MeV was assumed, but the calculated values beyond R_{50} were smaller than measured doses. However, since doses $< 50\%$ of the prescription dose have relatively little clinical significance, we considered the primary beam energy to be 6.72 MeV. Verhaegen et al. [18] found the same value for the primary beam energy after fine-tuning the 6 MeV electron beam from their Varian 2100C.

Cross-profiles were only modestly affected by the diameter and divergence assumed for the primary beam. The computed profile for $E_0 = 6.72$ MeV and FWHM = 0.13 cm agrees with measurement within statistical uncertainties ($\pm 2\%$). Thus, we considered the primary electrons incident on the foil to be parallel, mono-energetic at 6.72 MeV, and distributed within a circular area having a Gaussian radial distribution of 0.13 cm FWHM.

2.2 Optimal Beam Modifier

After the primary beam parameters had been determined, beam characteristics at 382 cm SSD were computed for beams modified by each of sets listed in Table I. They included cross-beam profiles, fluence intensities, x-ray contamination, and spectra. Figure 3 shows calculated electron fluence profiles along the x-axis (or y-axis) normalized per incident primary electron. In the absence of a flattening filter (*ED only*), beam intensity falls off rapidly with increasing distance from the axis. When large filters (20×20 cm²) are used, radiation intensity exhibits maxima (horns) at about 40 to 60 cm from the beam axis, and falls off at larger distances. The performance of filters at a fixed position (at or near 100cm SSD) is primarily affected by their size. All the 12×12 cm² filters except for *BM4* seem to produce the best over-all beam flatness. Their beams remain almost completely flat up to 40 cm from the central axis, and drops by not more than 10% at distances exceeding 60 cm. The 15×15 cm² filter is also of interest, exhibiting horns of 5% at off-axis distance of about 50 cm, but produced lower dose rate than the others. Note that all filters investigated in this study were sufficiently thick so that they could not be penetrated by the incident electrons. Hence filters of this design can be made of any material having sufficient thickness to stop the beam.

As shown in Fig. 3, dose rate and uniformity substantially vary with the location and size of energy degraders. The energy degraders placed at 100 cm SSD produced higher dose rate than those at 54cm SSD. Due to the beam divergence, fewer electrons were stopped or back-scattered by the energy degrader placed at 100 cm SSD. Among the energy degraders placed at isocenter (100 cm SSD), superior uniformity was achieved by the one, barely blacking a jaw-shaped field size (40×40 cm²). Thus, we considered the beam modifier (*BM6*), consisting of a 12×12 cm² aluminum filter and a 40×40 cm² PMMA energy-degrader placed at isocenter, as optimal. It produces a higher dose rate and a more uniform beam throughout the central part of the field than the others.

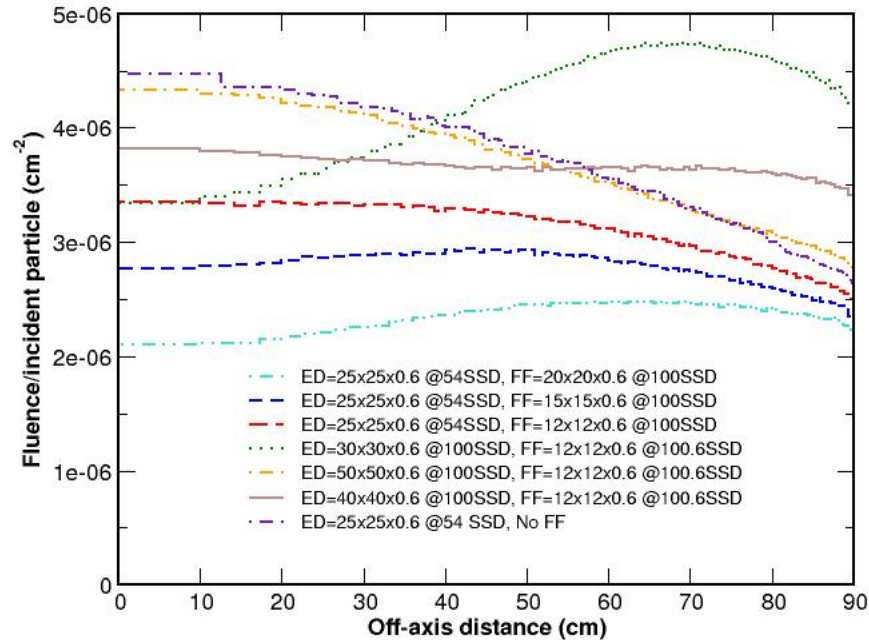


Figure 3. Monte Carlo-calculated beam profiles at 382 cm SSD for six sets of PMMA energy degraders and aluminum flattening filters, and for an energy degrader only (i.e., no flattening filter). In legend, ED and FF stand for energy degrader and flattening filter, respectively.

2.3 Monte Carlo Dosimetry of the TSEI System

Figure 4 compares MC-calculated stationary and rotational depth doses in a 15 cm-radius cylinder for four beam modifiers listed in Table I. All doses are normalized per incident primary electron. Without an energy degrader (*FF only*), considerable doses were delivered even beyond 2 cm-depth for both stationary and rotational irradiations, which indicates the necessity of energy degraders for our TSEI unit based on 6 MeV electron beams. The dose curves of energy-degraded modifiers are quite similar except that the beam modifiers placed at isocenter (*BM6*) yields higher dose rate than the others two (*BM2* and *BM3*). When the cylinder is rotated, the maximum dose occurs at or near the surface of the cylinder, whereas the depth of dose maximum in a stationary cylinder occurs at the beam axis at 0.65 cm-depth (with an energy degrader) or 1.0 cm-depth (without an energy degrader). The surface dose of a rotating cylinder is reduced to approximately 40% of that of a stationary cylinder, whereas our numerical calculations based on a semi-empirical formula in the literature [3] yielded a drop to 42%. These values and depth dose trends agree closely with the data measured by Podgorsak, et al. [3]. The drop in dose rate can be attributed to the larger SSD when a given point at the cylinder surface is rotated away from the beam axis, and the fact that electrons do not reach that point at all during half of each revolution.

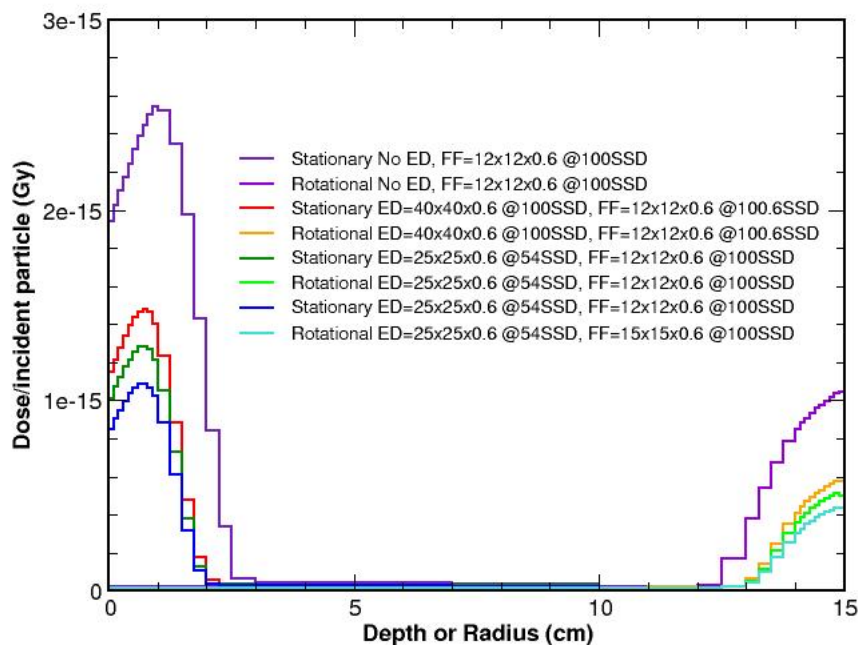


Figure 4. Monte Carlo-calculated doses for four beam modifiers, *BM2*, *BM3*, *BM6*, and *FF only* (see Table I for label). They were calculated assuming a water cylinder of 15 cm-radius and 50 cm-length, having its top (stationary dose) or side (rotational dose) surface perpendicular to the TSEI beams. Stationary doses vary from 0 cm to 15 cm in depth, while rotational doses from 15 cm to 0 cm in radius. The doses are normalized per incident particle. In legend, ED and FF stand for energy degrader and flattening filter, respectively.

3 CONCLUSIONS

Recent progress in computing power and Monte Carlo codes makes it practical to solve electron/photon transport problems in complex geometries using high speed personal computers (PCs). We took advantage of these advances to design the optimal energy degrader and flattening filter and to estimate patient doses in a setup for TSEI using the 6 MeV beam generated by a linear accelerator. The simulations showed a rapid falloff in beam intensity with increasing distance from the central axis, indicating that an external flattening filter was necessary. Also, it showed that a 0.6 cm-thick PMMA plate appropriately degraded beam energy so that patients rotating on a turntable receive over 95% of radiation dose to the 2 cm-layer skin. Dose rate and uniformity substantially varied with the location and size of beam modifiers.

Considering that our flattening filter and energy degrader were designed for a specific accelerator, beam energy and treatment distance, it is unlikely that identical devices would perform equally well under different operating conditions. Nevertheless, the basic design concept of beam modifiers, consisting of a PMMA energy degrader and an aluminum flattening

filter positioned at isocenter (*BM6*), should be adaptable for a wide variety of TSEI systems. The Monte Carlo techniques described in this paper can be generally applicable to other institutions that need the guideline of beam modifier design for TSEI. Further, Monte Carlo simulations can estimate the dosimetric performance of designed beam modifiers, thus eliminating the need of constructing and measuring a large number of devices that a purely experimental trial-and-error approach would entail.

4 ACKNOWLEDGMENTS

This work was gratefully initiated by Drs. Sharon Spencer and Ivan A. Brezovich at the UAB Comprehensive Cancer Center to improve dose uniformity on the patient's skin. The author acknowledges Dr. David W. O. Rogers at Carleton University, Canada for his corrections of our EGS4/DOSRZ input files. This work was made possible by EGS4 and its user codes, developed by Ionizing Radiation Standards Group at the National Research Council Canada and others.

5 REFERENCES

1. J. G. Trump, K. A. Wright, W. W. Evans, J. H. Anson, H. F. Hare, J. L. Fromer, G. Jacque, K. W. Horne, "High energy electrons for the treatment of extensive superficial malignant lesions," *Am. J. Roentgenol. Radium Ther. Nucl. Med.* **69**, pp.623-39 (1953).
2. AAPM, "Total skin electron therapy: technique and dosimetry," Report 23, *American Association of Physicists in Medicine* (December, 1987).
3. E. B. Podgorsak, C. Pla, M. Pla, P. Y. Lefebvre, and R. Heese, "Physical aspects of a rotational total skin electron irradiation," *Med. Phys.* **10**, pp.159-68 (1983).
4. C. Pla, R. Heese, M. Pla, and E. B. Podgorsak, "Calculation of surface dose in rotational total skin electron irradiation," *Med. Phys.* **11**, pp.539-46 (1984).
5. I. J. Das, J. F. Copeland, and H. S. Bushe, "Spatial distribution of bremsstrahlung in a dual electron beam used in total skin electron treatments: errors due to ionization chamber cable irradiation," *Med. Phys.* **21**, pp.1733-38 (1994).
6. J. A. Antolak and K. R. Hogstrom, "Multiple scattering theory for total skin electron beam design," *Med. Phys.* **25**, pp.851-59 (1998).
7. Z. Chen, A. G. Agostinelli, L. D. Wilson, and R. Nath, "Matching the dosimetry characteristics of a dual-field Stanford technique to a customized single-field Stanford technique for total skin electron therapy," *Int. J. Radiat. Oncol. Biol. Phys.* **59**, pp.872-85 (2004).
8. P. P. Kumar, U. K. Henschke, and J. R. Nibhanupudy, "Problems and solutions in achieving uniform dose distribution in superficial total body electron therapy," *J. Natl. Med. Assoc.* **69**, pp.645-47 (1977).
9. E. C. Pavón, F. Sánchez-Doblado, A. Leal, R. Capote, J. I. Lagares, M. Perucha, R. Arráns, "Total skin electron therapy treatment verification: Monte Carlo simulation and beam characteristics of large non-standard electron fields," *Phys. Med. Biol.* **48**, pp.2783-96

(2003).

10. W. R. Nelson, H. Hirayama, and D. W. O. Rogers, "The EGS4 code system," Report 265, *Stanford Linear Accelerator Center* (December, 1985).
11. D. W. O. Rogers, B. A. Faddegon, G. X. Ding, C. M. Ma, J. We, and T. R. Mackie, "BEAM: a Monte Carlo code to simulate radiotherapy treatment units," *Med. Phys.* **22**, 503-24 (1995).
12. A. F. Bielajew and D. W. O. Rogers, "PRESTA-The parameter reduced electron-step transport algorithm for electron Monte Carlo transport," *Nucl. Instrum. Methods Phys. Res.* **B18**, 165-81 (1987).
13. C.-M. Ma, P. Reckwerdt, M. Holmes, D. W. O. Rogers, B. Geiser, and B. Walters, "DOSXYZ users manual," NRCC Report No. PIRS-0509B (NRCC, Ottawa, Canada, 1996).
14. D. W. O. Rogers, I. Kawrakow, J. P. Seuntjens, B. R. B. Walters, and E. Mainegra-Hing, "NRC User Codes for EGSnrc," NRCC Report No. PIRS-702 (RevB) (NRCC, Ottawa, Canada, 2003).
15. A. Kapur, C.-M. Ma, E. Mok, D. Findley, and A. Boyer, "Monte Carlo calculations of electron beam output factors for a medical clinical accelerator," *Phys. Med. Biol.* **43**, 3479–94 (1998).
16. C.-M. Ma and S. Jiang, "Monte Carlo modelling of electron beams from medical accelerators," *Phys. Med. Biol.* **44**, R157–89 (1999).
17. D. Sheikh-Bagheri and D. W. O. Rogers, "Sensitivity of megavoltage photon beam Monte Carlo simulations to electron beam and other parameters," *Med. Phys.* **29**, 379–90 (2002).
18. F. Verhaegen, C. Mubata, J. Pettingell, A. M. Bidmead, I. Rosenberg, D. Mockridge, and A. E. Nahum, "Monte Carlo calculation of output factors for circular, rectangular, and square fields of electron accelerators (6–20 MeV)," *Med. Phys.* **28**, 938–49 (2001).
19. J. A. Antolak, M. R. Bieda, and K. R. Hogstrom, "Using Monte Carlo methods to commission electron beams: a feasibility study," *Med. Phys.* **29**, 771–86 (2002).
20. M. R. Bieda, J. A. Antolak, and K. R. Hogstrom, "The effect of scattering foil parameters on electron-beam Monte Carlo calculations," *Med. Phys.* **28**, 2527–34 (2001).